Identifying determinants of NADPH specificity in Baeyer–Villiger monooxygenases

Kamerbeek, Nanne M.; Fraaije, Marco W.; Janssen, Dick B.

Published in:
European Journal of Biochemistry

DOI:
10.1111/j.1432-1033.2004.04126.x

Publication date:
2004

Eur. J. Biochem. **271**, 2107–2116 (2004) © FEBS 2004 doi:10.1111/j.1432-1033.2004.04126.x

Identifying determinants of NADPH specificity in Baeyer–Villiger monooxygenases

Nanne M. Kamerbeek, Marco W. Fraaije and Dick B. Janssen

Laboratory of Biochemistry, Groningen Biomolecular Sciences and Biotechnology Institute, University of Groningen, the Netherlands

The Baeyer–Villiger monooxygenase (BVMO), 4-hydroxyacetophenone monooxygenase (HAPMO), uses NADPH and O_2 to oxidize a variety of aromatic ketones and sulfides. The FAD-containing enzyme has a 700-fold preference for NADPH over NADH. Sequence alignment with other BVMOs, which are all known to be selective for NADPH, revealed three conserved basic residues, which could account for the observed coenzyme specificity. The corresponding residues in HAPMO (Arg339, Lys439 and Arg440) were mutated and the properties of the purified mutant enzymes were studied. For Arg440 no involvement in coenzyme recognition could be shown as mutant R440A was totally inactive. Although this mutant could still be fully reduced by NADPH, no oxygenation occurred, indicating that this residue is crucial for completing the catalytic cycle of HAPMO. Characterization of several Arg339 and Lys439 mutants revealed that these residues are indeed both involved in coenzyme recognition. Mutant R339A showed a largely decreased affinity for NADPH, as judged from kinetic analysis and binding experiments. Replacing Arg339 also resulted in a decreased catalytic efficiency with NADH. Mutant K439A displayed a 100-fold decrease in catalytic efficiency with NADPH, mainly caused by an increased K_m. However, the efficiency with NADH increased fourfold. Saturation mutagenesis at position 439 showed that the presence of an asparagine or a phenylalanine improves the catalytic efficiency with NADH by a factor of 6 to 7. All Lys439 mutants displayed a lower affinity for $AADP^+$, confirming a role of the lysine in recognizing the 2′-phosphate of NADPH. The results obtained could be extrapolated to the sequence-related cyclohexanone monooxygenase. Replacing Lys326 in this BVMO, which is analogous to Lys439 in HAPMO, again changed the coenzyme specificity towards NADH. These results indicate that the strict NADPH dependency of this class of monooxygenases is based upon recognition of the coenzyme by several basic residues.

Keywords: 4-hydroxyacetophenone monooxygenase; flavoprotein; Baeyer–Villiger monooxygenase; NADPH; coenzyme specificity.

An intriguing phenomenon in enzymology is the discrimination that pyridine nucleotide-dependent enzymes can make between NADP(H) and NAD(H). The only difference between these two molecules is a phosphate group esterified with the 2′-hydroxyl group of the adenosine ribose. Phosphorylation of NAD^+, yielding $NADP^+$, is catalyzed by NAD kinase [1]. This allosteric enzyme, inhibited by NADPH and NADH, is thought to be the key enzyme in regulating the NAD^+ and $NADP^+$ levels in living cells. In general, oxidative degradation pathways use NAD^+ as an electron acceptor, whereas reductive biosynthesis routes primarily use NADPH as a source of reducing equivalents [2]. For biodegradation of xenobiotic compounds, this general rule is not valid as the monooxygenases and dioxygenases involved can be both NADPH and NADH specific.

NAD(P)(H)-dependent enzymes are ubiquitous, and, from a large number of X-ray structures, more than 10 different NAD(P)(H) binding folds can be identified, of which the Rossmann-fold is the most common [3]. A recent study of enzyme–NAD(P)(H) complexes showed that the binding fold also correlates with the conformation of the NAD(P)(H) ligand [4]. The affinity for NAD(P)(H) can range from very tight binding, as in nicotinoproteins, which use the nucleotides as a cofactor [5], to weak binding, as is the case for *p*-hydroxybenzoate hydroxylase, an enzyme that does not have a recognizable NAD(P)H-binding domain [6]. Although most enzymes are specific for one of the pyridine nucleotide coenzymes, there are also enzymes that display a dual specificity. For example, glutamate dehydrogenases form a family whose members have a specificity range from strict $NADP^+$ to strict NAD^+, including members that can use either coenzyme [7,8].

The molecular basis for coenzyme specificity has been studied for different classes of enzymes [9–14]. Furthermore,

Correspondence to M. W. Fraaije, Laboratory of Biochemistry, Groningen Biomolecular Sciences and Biotechnology Institute, University of Groningen, Nijenborgh 4, 9747 AG, Groningen, the Netherlands. Fax: + 31 50 3634165, Tel.: + 31 50 3634345, E-mail: m.w.fraaije@chem.rug.nl

Abbreviations: BVMO, Baeyer–Villiger monooxygenase; CFE, cell-free extract; CHMO, cyclohexanone monooxygenase; FMO, flavin-containing monooxygenase; HAPMO, 4-hydroxyacetophenone monooxygenase; NMO, N-hydroxylating monooxygenase; TrxR, thioredoxin reductase; WT, wild type.

Enzymes: cyclohexanone monooxygenase (EC 1.14.13.22); 4-hydroxyacetophenone monooxygenase (EC 1.14.13.x).

(Received 27 January 2004, revised 19 March 2004, accepted 30 March 2004)

examples of successful reversal of coenzyme specificity have been described for members of the dehydrogenase/reductase families (e.g. glutathione reductase [15], isopropyl-malate dehydrogenase [16], lactate dehydrogenase [17], formate dehydrogenase [18] and 2,5-diketo-D-gluconic acid reductase [19]). All of these enzymes contain a well-defined NADPH-binding domain. Recently, a reversal of coenzyme specificity for *p*-hydroxybenzoate hydroxylase, a member of the NAD(P)H-dependent flavoprotein aromatic hydroxylases, was also established [20]. In general, the removal or introduction of basic residues that interact with the 2′-phosphate of NADP(H), in combination with other mutations, is important for conversion of the coenzyme specificity [21].

Baeyer–Villiger monooxygenases (BVMOs) are flavoprotein monooxygenases that catalyze the conversion of a ketone into an ester or of a cyclic ketone into a lactone [22]. They are involved in oxidative degradation processes and biosynthesis of secondary metabolites, such as aflatoxin. The electrons required for catalyzing Baeyer–Villiger reactions are delivered by NADH or NADPH. BVMOs have been classified into two groups: Type I BVMOs contain FAD as a cofactor and use NADPH as the coenzyme, whereas Type II BVMOs are dependent on FMN and NADH [23]. While no Type II BVMO has been cloned, the number of cloned and characterized Type I BVMOs is steadily increasing [22]. Annotation of novel Type I BVMO sequences from the genome databases is possible using a specific sequence motif [24], and diverse PCR-based techniques provide tools to identify putative BVMOs from unsequenced organisms [25,26]. Type I BVMO sequences contain two dinucleotide-binding sequence motifs (Rossmann-fold motifs) – GxGxxG – which are involved in binding of the ADP moieties of FAD and NADPH [27]. This distinguishes them from another class of flavin-containing monooxygenases – the mechanistically related aromatic hydroxylases (such as *p*-hydroxybenzoate hydroxylase) – which contain only one dinucleotide-binding domain for FAD binding [6]. The overall sequence organization in Type I BVMOs is similar to the organization in the NAD(P)H-dependent disulfide reductases [28], and is also found in two other flavoprotein monooxygenase families, namely flavin-containing monooxygenases (FMOs) and N-hydroxylating monooxygenases (NMOs). Type I BVMOs, FMOs and NMOs have been shown to form one superfamily [24]. The individual members of this monooxygenase superfamily are all single-component, FAD-containing enzymes and prefer NADPH as the electron donor. At present, there is no structure known of any BVMO, FMO or NMO.

BVMOs are of industrial interest as they show broad substrate specificities and high enantio- and regioselective conversions [22,23,29,30]. The most extensively studied BVMO, cyclohexanone monooxygenase (CHMO), has been shown to convert over 100 unnatural substrates. This has fuelled a biotechnological interest in this class of monooxygenases. For isolated enzyme applications, a change of an NADPH-specific BVMO towards an NADH utilizing enzyme is economically attractive, as NADH is less expensive and more stable than NADPH. To circumvent expensive coenzyme recycling, whole-cell conversions, using recombinant *Escherichia coli*, are often favored for enzyme-mediated oxygenating reactions [31,32]. Also for these whole-cell conversions, BVMOs that (also) accept NADH as a coenzyme would be beneficial for catalytic efficiency, as *E. coli* contains high levels of NADH [33]. Until the present study, no BVMO had been investigated to identify amino acids responsible for its coenzyme specificity.

Recently, we cloned the gene encoding 4-hydroxyacetophenone monooxygenase (HAPMO) from *Pseudomonas fluorescens* ACB into *E. coli*. The enzyme, a 145 kDa dimer containing one FAD molecule per subunit, efficiently catalyzes Baeyer–Villiger oxidation reactions on various ketones. Besides Baeyer–Villiger oxidations, the enzyme also catalyzes highly enantioselective sulfoxidations with the use of NADPH [34]. In a previous study where we analyzed the primary HAPMO sequence, we identified an arginine (Arg339) that was strictly conserved among the known Type I BVMOs [35]. This arginine is located close to the C-terminal Rossmann-fold motif, which is involved in NADPH binding. We suggested that this residue is involved in the recognition of NADPH, as it also aligns with a conserved basic residue in yeast FMO (Lys219) that was shown to contribute to coenzyme recognition [36]. In the present work we explored, by site-directed mutagenesis, whether Arg339 is involved in coenzyme recognition by HAPMO. Two other conserved basic amino acids were also examined regarding their contribution to coenzyme specificity. In addition, another BVMO (CHMO) was included in this site-directed mutagenesis study.

Materials and methods

Chemicals

NADPH, NADH, $NADP^+$, 3-aminopyridine adenine dinucleotide phosphate ($AADP^+$), 3-acetylpyridine adenine dinucleotide phosphate (acetyl-$NADP^+$), thionicotinamide adenine dinucleotide phosphate (thio-$NADP^+$), 4-hydroxyacetophenone, cyclohexanone, and L(+)-arabinose were obtained from Sigma-Aldrich.

Strains and plasmids

E. coli TOP10 cells were obtained from Invitrogen. For expression of HAPMO in *E. coli* TOP10 cells, a pBAD/*myc*-HisA vector (Invitrogen) with a unique *Nde*I site at the start of translation was created (pBAD*N*). For this, the two original *Nde*I sites were deleted by mutating the guanine base of the CATATG *Nde*I recognition sequence into a cytosine, and the unique *Nco*I site at the translation start was changed into a unique *Nde*I site by replacing the ACC sequence in front of the start codon by CAT. These mutations were introduced using the Quick-change site-directed mutagenesis kit from Stratagene. The *hapE* gene was cloned into *Nde*I and *Bgl*II digested pBAD*N* yielding pBAD/*hapE. E. coli* TOP10, harboring plasmid pQR239 encoding the cyclohexanone monooxygenase from *Acinetobacter* sp. NCIB 9871 [38], was kindly provided by J. Ward (University College London). Cells were grown in Luria–Bertani (LB) broth supplemented with ampicillin (100 $\mu g \cdot mL^{-1}$) (LB_{amp}).

Site-directed and random mutagenesis

The Quick-change site-directed mutagenesis kit from Stratagene was used for the construction of mutants, using the plasmid pBAD/*hapE* as template and the following mutagenic primers (the letters f and r, at the end of the primer name denote forward or reverse primer, respectively): PR339Af, 5′-GAAGGTCTTTGCGGCGACCACCAA CTG-3′ and PR339Ar, 5′-CAGTTGGTGGTCGCCGC AAAGACCTTC-3′; PK439Af, 5′-CCTGTCGGCGGT GCGCGCATCGTACGAG-3′ and PK439Ar, 5′-CTCG TACGATGCGCGCACCGCCGACAGG-3′; PR440Af, 5′-GTCGGCGGTAAGGCGATCGTACGAGATAAC-3′ and PR440Ar, 5′-GTTATCTCGTACGATCGCCTTAC CGCCGAC-3′. The underlined bases indicate the bases that were altered to create an alanine codon.

For saturation mutagenesis at position 439, a modified procedure of Stratagene was followed. After the first transformation of the *E. coli* TOP10 cells with the PCR mixture, the resulting colonies were pooled and their plasmids isolated. These plasmids were used for an additional transformation step to remove hybrid plasmids. The following primers were used: PK439XfII, 5′-CCTGTCGGCGGTNN(G/C)CGCATCGTACGAG-3′ and PK439XrII, 5′-CTCGTACGATGCG(G/C)NNAC CGCCGACAGG-3′. Transformants were picked and grown overnight in 96-well plates containing LB_{amp} + 10% (v/v) glycerol and then stored at −80 °C until required.

The mutation K326A in CHMO was created using the primers PK326Af, GATTTGTATGCAGCGCGTC CGTTGTG and PK326Ar, CACAACGGACGCGCTGC ATACAAATC (the underlined bases indicate the bases altered to create an alanine codon) and pQR239 [38] as template.

Screening of the saturation mutagenesis library

The 200 clones from the library were cultured individually overnight at room temperature in tubes containing 5 mL of LB_{amp} + 0.002% (w/v) arabinose. After harvesting by centrifugation, the cells were resuspended in 0.5 mL of potassium phosphate buffer (pH 7.5), then sonicated and centrifuged to produce cell-free extract (CFE). NADPH or NADH consumption by CFE in the presence of 4-hydroxyacetophenone was monitored for 5 min at 370 nm using a plate reader (Bio-Tek instruments). Per well, the reaction mixtures were as follows: 190 μL of potassium phosphate buffer (pH 7.5), 400 μM 4-hydroxyacetophenone, 1 mM NADPH or NADH, and 10 μL of CFE. The reaction was started by the addition of CFE. The protein content of the CFEs was measured using the Bradford assay [39].

Expression and purification of wild-type HAPMO and mutant enzymes

E. coli TOP10 cells containing the plasmids with the mutated genes were precultured in 30 mL of LB_{amp} for 6–8 h at 30 °C. The preculture was used to inoculate 1 L of LB_{amp} + 0.002% (w/v) arabinose. The cells were grown overnight at 20 °C to a final attenuance (D), at 600 nm, of 2–3, and harvested by centrifugation. Further purification steps were performed as described previously [35]. HAPMO concentrations were determined spectrophotometrically using a molar extinction coefficient of 12.4 $mM^{-1}\cdot cm^{-1}$ at 439 nm for protein-bound FAD [35].

Expression and purification of wild-type CHMO and mutant enzymes

E. coli TOP10 cells, containing plasmid pQR239 or plasmid pQR239/K326A, were precultured in 30 mL of LB_{amp} for 6–8 h at 30 °C. The preculture was used to inoculate 1 L of LB_{amp} + 0.01% (w/v) arabinose. The cells were grown overnight at 37 °C, harvested by centrifugation and resuspended in 20 mM potassium phosphate buffer, pH 7.2. Cells were sonicated and then centrifuged (15 000 ***g*** for 30 min at 4 °C). Subsequently, CHMO was partially purified from the cell-free extract using two chromatography steps. The supernatant was loaded onto a Hi-prep 16/10Q XL DEAE-sepharose (50 mL) column (Pharmacia) that was pre-equilibrated with 20 mM potassium phosphate buffer containing 1 mM mercaptoethanol. Protein was eluted from the column with a linear gradient of 0–0.5 M KCl in 20 mM phosphate buffer, pH 7.2, in five column volumes. Fractions containing CHMO activity were pooled and concentrated using an Amicon filtration unit equipped with a 30 kDa cut-off filter. Concentrated protein was applied on a Superdex 200 26/60 size-exclusion column (Pharmacia). The protein was eluted with 20 mM potassium phosphate buffer, pH 7.2, containing 1 mM mercaptoethanol. Fractions containing CHMO activity were pooled and concentrated. The CHMO concentration was determined using an extinction coefficient of 13.8 $mM^{-1}\cdot cm^{-1}$ at 440 nm [40].

Protein and activity assays

All HAPMO activity measurements were performed in air-saturated 50 mM potassium phosphate buffer, pH 7.5. The Michaelis–Menten constants, k_{cat} and K_m, for NADPH and NADH were determined by varying the concentrations of the coenzyme in the presence of 100 μM 4-hydroxyacetophenone. Enzyme activities were determined spectrophotometrically at 25 °C by following, at 370 nm, the absorbance decrease caused by NAD(P)H oxidation (ε_{370} = 2.7 $mM^{-1}\cdot cm^{-1}$). In the case of high K_m values for NADPH and/or NADH, the absorbance decrease was followed at 390 nm (ε_{390} = 0.43 $mM^{-1}\cdot cm^{-1}$).

CHMO activity was determined by monitoring the oxidation of NADPH upon conversion of 100 μM cyclohexanone in 0.1 M glycine/NaOH, pH 9.0.

$AADP^+$ titrations

UV/Vis spectra were acquired at 25 °C using a Perkin Elmer Lambda Bio40 spectrophotometer. Aliquots of the concentrated $AADP^+$ solution were added to the enzyme solution until saturation was observed. Absorbance changes were plotted as difference spectra and, from these spectra, the changes at selected wavelengths were used to calculate the binding stoichiometry at each step of the titration. As $AADP^+$ also absorbs, to some extent, up to 400 nm, absorbance differences were typically taken from the

Table 1. Kinetic analysis of wild-type 4-hydroxyacetophenone monooxygenase (WT-HAPMO), HAPMO mutants, WT cyclohexanone monooxygenase (CHMO) and CHMO mutant K326A.

	k_{cat} (s^{-1})		K_m (μM)		k_{cat}/K_M ($s^{-1}\cdot mM^{-1}$)		NADPH/ NADH	K_d AADP$^+$ μM	FAD_{ox}[a] + N %	FAD_{ox}[b] + N + H %
	NADPH	NADH	NADPH	NADH	NADPH	NADH				
HAPMO										
WT	10.1 ± 0.1	1.7 ± 0.2	12 ± 0.6	1440 ± 140	840	1.2	700	0.4	0	46
R339A	> 0.1	0.19 ± 0.1	> 3000	3000 ± 1860	0.0003	0.063	4.8×10^{-3}	> 50	77	96
K439A	1.6 ± 0.1	2.4 ± 0.1	200 ± 51	520 ± 80	8	4.6	1.7	2.1	25	38
K439F	1.0 ± 0.1	2.4 ± 0.2	80 ± 18	300 ± 80	13	8	1.7	2.5	20	50
K439P	0.2 ± 0.01	0.7 ± 0.1	17 ± 3.5	1280 ± 290	12	0.5	24	1.8	73	80
K439N	3.5 ± 0.2	5.1 ± 0.2	78 ± 10	780 ± 75	45	7	6	2.5	1	46
R440A	–	–	–	–	< 0.0001	< 0.0001	–	0.1	3	3
CHMO										
WT	14 ± 0.5	1.4 ± 0.1	7.3 ± 1.4	420 ± 80	1900	3.3	576			
K326A	3.7 ± 0.2	0.5 ± 0.1	160 ± 30	230 ± 100	23	2.2	10			

[a] FAD_{ox} + N indicates the percentage of oxidized cofactor present during the steady-state turnover of NADPH only. [b] FAD_{ox} + N + H indicates the percentage of oxidized cofactor present during steady-state turnover of NADPH in the presence of 4-hydroxyacetophenone.

450–500 nm region. From these data, the binding constants were obtained using Eqn (1).

$$K_d = \frac{[E]_{free} \cdot [AADP]_{free}}{[E \cdot AADP]} \quad (1)$$

Flavin-monitored turnover of HAPMO

The redox state of the flavin cofactor during catalysis was monitored on an Applied Photophysics SX17MV stopped-flow instrument. All concentrations stated are those in the reaction chamber after mixing. For flavin-monitored turnover of HAPMO, equal amounts of air-saturated enzyme solution (10 μM) and substrate solution in 50 mM phosphate buffer, pH 7.5, containing 1.5 or 3 mM NADPH, with or without 500 μM 4-hydroxyacetophenone, were mixed. The redox state of the flavin was monitored, at 439 nm, over a 10 s timespan. The difference between the absorbance of FAD_{ox} and FAD_{red}, determined by mixing wild-type enzyme with buffer, without or with NADPH, respectively, was set as 100% oxidized FAD. When mutants could not be reduced completely in the presence of NADPH alone, the ratio of absorbance for FAD_{ox} and FAD_{red} from wild-type HAPMO (WT-HAPMO) was used to calculate the FAD_{red} absorbance for the mutant.

Results

Coenzyme specificity and coenzyme analogue binding for WT-HAPMO

HAPMO has a 700-fold preference for NADPH over NADH, as expressed by the ratio $(k_{cat}/K_{m(NADPH)})/(k_{cat}/K_{m(NADH)})$ (Table 1). To gain further insight into the coenzyme affinity of WT-HAPMO, we attempted to measure NADP$^+$ binding spectrophotometrically. It was expected that binding of NADP$^+$ would position the nicotinamide ring close to the oxidized isoalloxazine ring of the FAD cofactor. This change in the microenvironment of the cofactor is typically reflected by changes in the flavin spectral properties, as observed for NADP$^+$ binding to CHMO [40]. Such a change would allow us to determine the dissociation constant for NADP$^+$. Remarkably, WT-HAPMO did not show any perturbation of the flavin spectrum upon NADP$^+$ addition up to a concentration of 1.2 mM. This shows that NADP$^+$ is not binding, or at least not close to, the isoalloxazine moiety of the FAD. NADP$^+$ at a concentration of 500 μM did not inhibit HAPMO activity in the presence of 200 μM NADPH, indicating that the oxidized coenzyme does not compete strongly with its reduced form (Table 2).

In order to identify a suitable probe for coenzyme binding, three NADP$^+$ analogues were tested for their ability to inhibit HAPMO catalysis. Their structures differ from each other only in carrying different substituents on the positively charged nicotinamide ring (Fig. 1). From these compounds, only AADP$^+$ was found to be a very effective inhibitor, as 5 μM AADP$^+$ was sufficient to inhibit HAPMO activity by 80% (Table 2). This suggests that the substitutions on the 3-position of the pyridine ring are crucial for coenzyme binding. In contrast to NADP$^+$, titration of oxidized HAPMO with AADP$^+$ resulted in considerable changes to the flavin spectrum (Fig. 2). The absorbance change at 480 nm was used to calculate the dissociation constant (K_d) of AADP$^+$. The strong inhibi-

Table 2. Inhibition of 4-hydroxyacetophenone monooxygenase (HAPMO) activity by NADPH analogues. Activity was measured using 200 μM NADPH, 200 μM 4-hydroxyacetophenone and 0.05 μM HAPMO.

Analogue	Concentration (μM)	Activity (%)
–	–	100
NADP$^+$	500	100
Thio-NADP$^+$	500	96
Acetyl-NADP$^+$	500	65
AADP$^+$	5	20

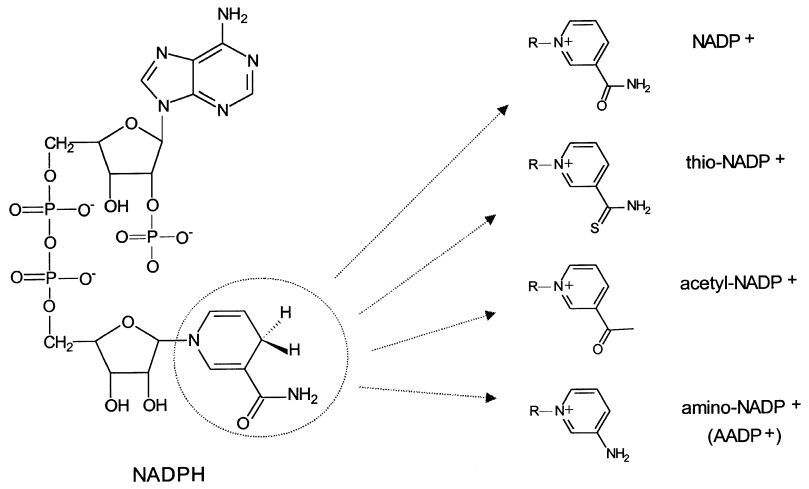

Fig. 1. Structures of NADPH, $NADP^+$ and $NADP^+$ analogues.

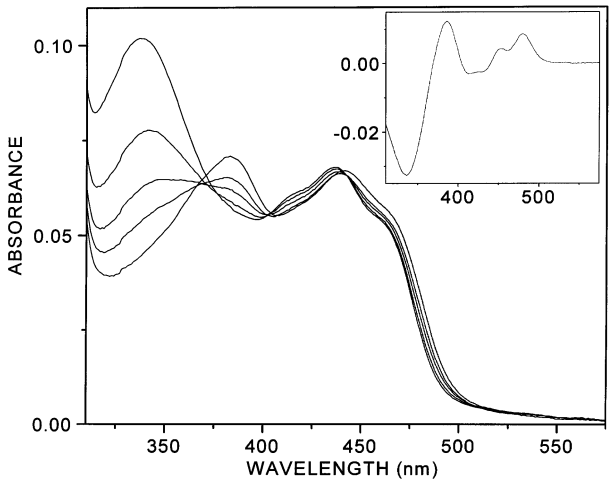

Fig. 2. $AADP^+$ titration of 4-hydroxyacetophenone monooxygenase (HAPMO). Spectra are shown of HAPMO K439A (6.2 μM) in the presence of 0, 3.4, 6.7, 10.0, 16.7 and 33.0 μM $AADP^+$. The increase in absorbance at ≈ 350 nm is mainly the result of $AADP^+$ absorbance. Absorbance changes at higher wavelengths are indicative of ligand binding. The inset shows the difference spectrum between uncomplexed enzyme and the spectrum obtained after addition of 13.4 μM $AADP^+$.

tion by $AADP^+$ is reflected by its low K_d, of only 0.4 μM (Table 1). Hence, $AADP^+$ was chosen as a probe to determine the coenzyme affinity of the HAPMO variants.

As mutagenesis of residues involved in binding of the coenzyme could also affect the efficiency of flavin reduction, WT-HAPMO was first studied to obtain insight into the equilibrium between reduced and oxidized FAD during steady-state catalysis. For this, the redox state of the flavin was followed spectrophotometrically during turnover. As expected, WT-HAPMO was completely reduced upon mixing with NADPH only. In the presence of 4-hydroxyacetophenone, the ratio FAD_{ox}/FAD_{red} during turnover was ≈ 1 : 1 (Table 1), suggesting a balance between the reductive and oxidative half-reactions.

Mutagenesis of conserved residues and characterization of the mutants

In order to identify amino acids that could account for the strict NADPH specificity, the HAPMO sequence was aligned with the sequences of other characterized Type I BVMOs (Fig. 3). The sequence-related yeast FMO was also included because the conserved arginine of Type I BVMOs (HAPMO R339), aligns with Lys219 of yeast FMO, a residue known to be involved in NADPH recognition [36]. Furthermore, part of the sequence of the *E. coli* thioredoxin reductase (TrxR), for which the structure has been determined, could be aligned. The crystal structure of *E. coli* TrxR, in complex with $AADP^+$ (Protein Data Bank entry 1F6M), has revealed that residues Arg177 and Arg182 interact with the 2′-phosphate moiety of the NADPH analogue [41]. As shown in Fig. 3, HAPMO R339 aligns with TrxR R177. There is no obvious HAPMO counterpart for TrxR Arg182. Usually, the 2′-phosphate interacts with two or three basic residues in combination with a serine or another amino acid containing an OH-group [20,42]. Two additional conserved basic residues, which might contribute to this, were identified in the BVMO sequences (HAPMO Lys439 and Arg440).

To study the involvement of Arg339, Lys439 and Arg440 in coenzyme specificity, these positively charged amino acids were individually replaced with an alanine. All variants appeared as dimers upon purification and contained one FAD per enzyme monomer, as derived from the ratio A_{280}/A_{440}. Apparently, the mutations do not affect dimerization and FAD binding. To examine the effect of the mutations on coenzyme specificity, the k_{cat} and K_m values for NADPH and NADH were determined and compared with those of WT-HAPMO (Table 1).

Properties of R339A. Replacement of Arg339 with alanine had a dramatic effect on catalysis. The specificity shifted 150 000-fold towards NADH. However, this shift was mainly caused by an almost complete loss of activity with NADPH and not by improvement of activity with NADH. Whereas WT-HAPMO displays a high affinity for $AADP^+$, titration of the R339A enzyme with up to 50 μM $AADP^+$ did not lead to significant spectral perturbation of the FAD

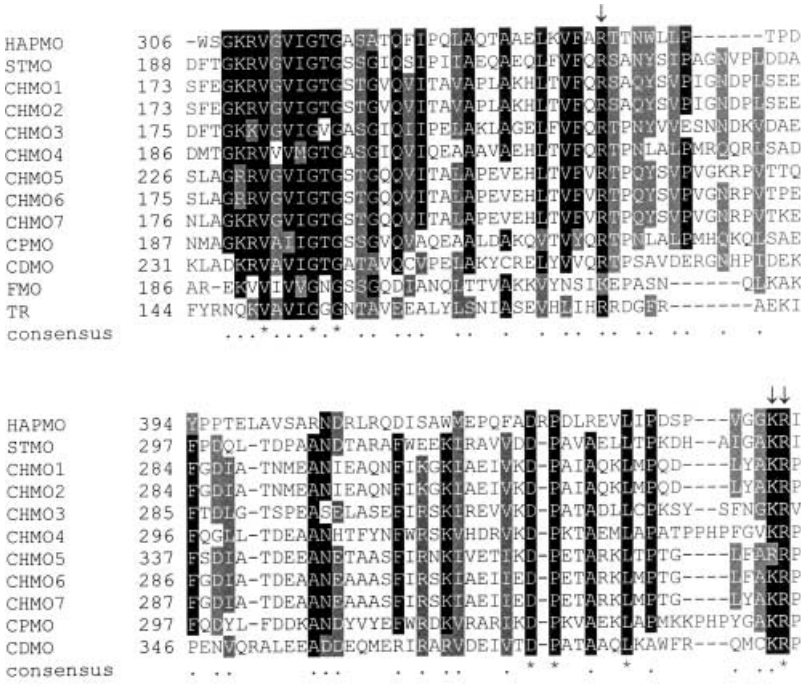

Fig. 3. Partial alignment of cloned Type I Baeyer–Villiger monooxygenases (BVMOs), yeast flavin-containing monooxygenase (FMO) and *Escherichia coli* thioredoxin reductase. The arrows indicate the mutated amino acids.

spectrum. This low affinity for $AADP^+$ is in agreement with the observed high K_m value for NADPH for R339A, being > 3 mM. Next, mutant R339A was studied using flavin-monitored turnover experiments to examine whether coenzyme recognition is indeed limiting catalysis. Mixing R339A with NADPH, in the presence or absence of 4-hydroxyacetophenone, showed that the majority of FAD is in the oxidized state during turnover. This suggests that NADPH-mediated flavin reduction is rate limiting for this mutant.

Properties of K439A. The K439A mutation resulted in a 400-fold improvement of preference towards NADH. This was mainly caused by an increased K_m for NADPH. The reduced recognition of NADPH was also reflected in a higher K_d of $AADP^+$ for K439A. Interestingly, except for a decreased efficiency with NADPH, an improvement of catalytic efficiency with NADH was also observed. Mutagenesis of Lys439 did not drastically change the balance between reduced and oxidized flavin during steady-state turnover, indicating that the reactivity with the flavin is not impaired by this mutation.

Properties of R440A. Mutagenesis of Arg440 resulted in a drastic effect on catalysis, with no significant activity being observed for this mutant (Table 1). To our surprise, the R440A mutant showed slightly enhanced binding of $AADP^+$ compared with WT-HAPMO. The inactivity of this mutant suggests that NADPH could still bind to this mutant, but that the reduction of FAD or subsequent steps were impaired, preventing turnover. The flavin-monitored turnover data showed that R440A could indeed be fully reduced by NADPH (Table 1). However, in the presence of the aromatic substrate, all the flavin remained in the reduced state, indicating that subsequent steps towards oxygenation are impaired. Together, these results show that Arg440 is not important for coenzyme recognition, but plays an important role in catalysis.

Saturation mutagenesis on K439

The site-directed mutagenesis study revealed that Lys439 is an attractive target for mutagenesis to change the HAPMO coenzyme preference towards NADH. To investigate whether the improved efficiency with NADH, obtained with K439A, could be further improved by substitution with other amino acids, it was decided to perform saturation mutagenesis to create every possible amino acid substitution at position 439. From a library of 200 clones, CFEs were prepared and measured for their specific activities with NADPH and NADH. As controls, CFEs of *E. coli* expressing WT-HAPMO and K439A were included in these experiments.

Interestingly, almost half of the 200 clones (48%) showed a higher activity with NADH compared to WT-HAPMO, and 19% of the clones displayed an activity within the K439A range (Fig. 4). Four clones with increased activity relative to K439A were sequenced, and three different substitutions – K439F, K439P and K439N – were identified. The three mutants were purified and tested for their kinetic parameters (Table 1). The K439P mutant was apparently false-positive, as it showed similar K_m values but significantly lower k_{cat} values with both coenzymes compared to WT-HAPMO. As expected, both K439F and K439N displayed improved catalytic efficiencies with NADH. Mutant K439F showed a similar shift in coenzyme preference as K439A compared with WT-HAPMO. However, the K439F mutant displayed relatively low K_m values for both NADPH and NADH, resulting in relatively high catalytic efficiencies for both coenzymes. Compared to the K439A and K439F mutants, the K439N variant displayed a relatively high k_{cat} value with NADH (5.1 s^{-1}), approaching the k_{cat} of WT-HAPMO with NADPH (10.1 s^{-1}).

In line with the increased K_m values for NADPH, the K_d values for $AADP^+$ of all three Lys439 variants increased significantly when compared with WT-HAPMO (Table 2).

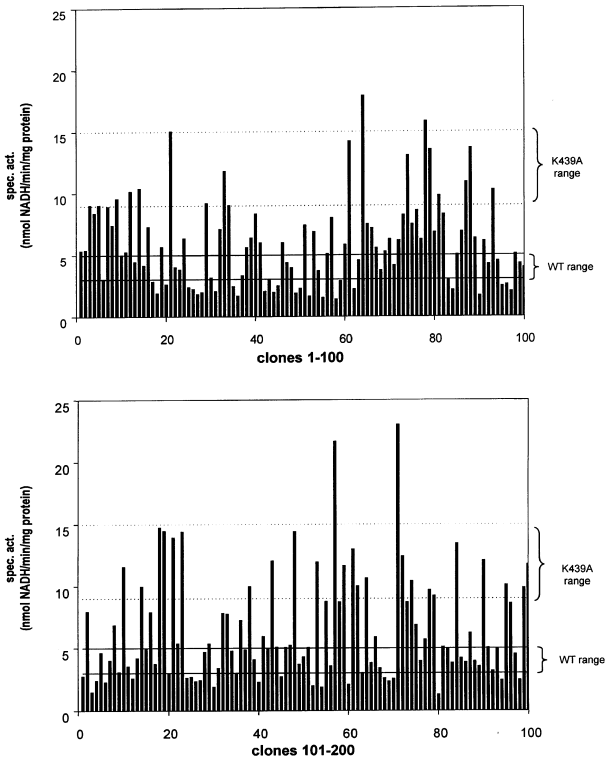

Fig. 4. Specific activities with NADH for the clones from the K439X library. The selected clones are indicated with arrows. The unbroken and dotted lines indicate the range of wild-type (WT) and K439A activities found, respectively.

This again confirms a role of Lys439 in coenzyme binding. By monitoring the redox state of the flavin during turnover of NADPH, it was found that the different amino acid substitutions at position 439 have different effects on the efficiency of flavin reduction by NADPH. Only the K439N mutant was fully reduced by NADPH. In the presence of 4-hydroxyacetophenone and NADPH, it was found that the K439A/F/N mutants showed $[FAD_{ox}]/[FAD_{red}]$ ratios of around 1/1 during steady-state catalysis, which is also the case for WT-HAPMO. The K439P mutant was less efficient in the reductive half-reaction, while it was able to bind NADPH, as evidenced by $AADP^+$ binding. This suggests that with this HAPMO variant, NADPH binding is perturbed in such a way that hydride transfer is impaired. This is also reflected in the low k_{cat} values observed for this mutant. Apparently all other engineered Lys439 mutants are still able to bind the coenzyme in such a way that the nicotinamide ring is correctly positioned to facilitate flavin reduction, resulting in acceptable k_{cat} values.

K326A mutation in CHMO

As mutating the conserved Lys439 in HAPMO drastically changed the recognition of coenzyme, it was expected that a similar effect could be obtained when mutating an analogous residue in another Type I BVMO. To test this hypothesis, Lys326 in CHMO was mutated to alanine. Kinetic analysis of the K326A mutant again revealed a significant shift in coenzyme specificity towards NADH (Table 2). As with HAPMO, the catalytic efficiency with NADPH was reduced by two orders of magnitude, mainly owing to an increased K_m for NADPH. In contrast with the results obtained with HAPMO K439A, there was also a slight decrease in the catalytic efficiency with NADH. Nevertheless, these results confirmed our finding that the respective conserved lysine in Type I BVMOs is involved in recognition of the coenzyme.

Discussion

BVMOs are flavin-containing monooxygenases that catalyze NAD(P)H-dependent oxygenations of a variety of substrates. Two classes of BVMOs have been described: Type I BVMOs, which are FAD and NADPH dependent; and Type II BVMOs, which are FMN and NADH dependent. The current report describes a mutagenesis study of three basic residues within the Type I BVMO class, in order to elucidate their possible role in coenzyme recognition.

Sequence analysis has shown that HAPMO contains two Rossmann-fold domains; one is responsible for FAD binding (N-terminal domain) and the other is responsible for binding the coenzyme, NADPH (C-terminal domain). HAPMO, showing a 700-fold preference for NADPH over NADH, contains a conserved arginine (Arg339), located 19 residues after the C-terminal Rossmann-fold motif (GxGxxG). It was shown by Suh *et al.* that mutation of the homologous Lys219, in the distantly related yeast flavin-dependent monooxygenase, to an alanine, resulted in a 90-fold reduction of activity with NADPH, whereas the activity with NADH was unaffected [36]. Changing HAPMO Arg339 to alanine had a detrimental effect on the catalytic efficiency with NADPH, as it showed a decrease of six orders of magnitude. In fact, the K_m for NADPH could not be determined, as no saturation behavior was observed at the concentrations measured, suggesting loss of coenzyme recognition. This was supported by the dramatically decreased affinity of the $NADP^+$ analogue, $AADP^+$. Activity with NADH was also impaired, but to a lesser extent (20-fold). From these results it can be concluded that Arg339 in HAPMO is crucial for coenzyme binding.

Besides arginines, also lysines are often found to interact with the 2′-phosphate group of NADPH [43–46]. We have found that the conserved lysine, at HAPMO position 439, clearly contributes to the discrimination between NADPH and NADH. The introduction of an alanine at this position allows improved catalytic performance with NADH, while the catalytic efficiency with NADPH is significantly affected. Replacing the analogous lysine (Lys329) in another Type I BVMO, CHMO, again resulted in a shift of coenzyme preference. This is in line with the fact that all characterized Type I BVMOs are highly selective for NADPH, and all contain a lysine or arginine at this position. By saturation mutagenesis it was probed which mutation would give the highest activity with NADH for HAPMO. Introduction of a phenylalanine gives the best result in terms of catalytic efficiency, as it was increased sevenfold when compared with WT-HAPMO. The highest k_{cat} value with NADH (5.1 s^{-1}) was obtained with the K439N variant. Apparently, relatively bulky residues have to replace the lysine residue to retain productive coenzyme binding.

It was found that Arg440 does not play a role in coenzyme recognition, but instead is important for a specific catalytic event. The tight binding of $AADP^+$, and the reduction by NADPH without detectable turnover, indicate that Arg440 is involved in facilitating a reaction step after the reduction of the FAD cofactor. A possible role for this residue could be the stabilization of the flavin–peroxide intermediate formed upon reaction of the reduced FAD with molecular oxygen. The role of Arg440 might also resemble the function of Arg66 in human glutathione reductase where it is postulated that this residue has electrostatic interactions with the formed $NADP^+$ so that it is repelled from the isoalloxazine environment [47]. However, mutant R440A does not show tighter binding of $NADP^+$ compared to WT-HAPMO (data not shown).

The results obtained show that HAPMO is able to distinguish between NADPH, $NADP^+$ and $AADP^+$. The differences in affinity must be related to the properties of the nicotinamide moiety. The reduced nicotinamide ring of NADPH is neutral, nonaromatic and slightly shaped into a boat nonplanar conformation [48]. Typically, the carboxamide side-chain is bound in the enzyme active site via one or more hydrogen bonds [49]. Upon oxidation, the nicotinamide ring becomes positively charged and aromatic. This change could influence the binding properties of coenzyme to the enzyme and would therefore explain why $NADP^+$ binds with such low affinity to HAPMO. Similar results have been observed with dihydrofolate reductase, which binds NADPH much more tightly compared to $NADP^+$ [50]. What remains obscure is why, in contrast to HAPMO, CHMO is able to bind $NADP^+$ relatively tightly, with a K_d of 32 μM [40]. $NADP^+$ has also been shown to be a competitive inhibitor to NADPH for CHMO, with a reported K_i of 38 μM [51]. However, we have found that $NADP^+$ is not an effective inhibitor for HAPMO. The apparent differences in $NADP^+$ binding will only be resolved when more structural information on BVMOs becomes available. The remarkable difference between the binding of $NADP^+$ and $AADP^+$ by HAPMO shows that the side-chain of the nicotinamide ring plays a delicate role. It appears that $NADP^+$, having a relatively bulky carboxamide side-chain at the nicotinamide ring, is sterically hindered to bind properly, while $AADP^+$, containing an amine side-chain, is able to bind tightly. Comparable studies with $NADP^+$ analogues on the glutamate synthase β subunit also showed that the size of the substituent at the 3′ position determines the strength of ligand binding [52]. A major part of the HAPMO sequence (residues 143–339) shares 23% sequence identity with TrxR [24], suggesting that the structure of Type I BVMOs will, to some extent, share structural features with this FAD-containing NADPH-dependent oxidoreductase. The involvement of Arg339 in NADPH recognition, and the efficient binding of $AADP^+$, are in agreement with this hypothesis. Inspection of the TrxR structure complexed with $AADP^+$ hints to a possible reason for the extremely tight binding of the $NADP^+$ analog. The structure reveals a hydrogen bond between the 3-amine group of the coenzyme analog and the O_4 of the isoalloxazine ring of the flavin cofactor, which would specifically promote $AADP^+$ binding. Such a ligand–cofactor interaction is in line with the observation that another Type I BVMO, showing relatively low sequence identity with HAPMO (24%), is also efficiently inhibited by $AADP^+$ [53]. The homology of HAPMO with TrxR also suggests that NADPH binds on the *re* side of the flavin. This is in line with the finding of Manstein *et al*., that NADPH also binds at the *re* side of FAD in CHMO [54].

To conclude, we have identified two conserved basic amino acids within the family of the Type I BVMOs that account for their NADPH specificity. Furthermore, we have constructed HAPMO mutants that display a significantly increased activity with NADH. However, owing to the relatively high K_m values, these enzyme variants are still not efficient enough to be used for biocatalytic applications. For a complete reversal of the coenzyme specificity of a Type I BVMO, in terms of catalytic efficiency, apparently a greater number of residues need to be mutated. Elucidation of a crystal structure of a Type I BVMO would greatly facilitate such an enzyme redesign approach.

Acknowledgements

This research was funded by the Council for Chemical Sciences of the Netherlands Organization for Scientific Research (CW-NWO), division 'Procesvernieuwing voor een schoner milieu'. We thank Dr Willem van Berkel for critical reading of the manuscript.

References

1. Kawai, S., Mori, S., Mukai, T., Hashimoto, W. & Murata, K. (2001) Molecular characterization of *Escherichia coli* NAD kinase. *Eur. J. Biochem.* **268**, 4359–4365.
2. Moat, G.A. & Foster, J.W. (1987) Biosynthesis and salvage pathways of pyridine nucleotides. In *Pyridine Nucleotide Coenzymes Part B* (Dolphin, D., Poulson, R. & Avramovic, A., eds), pp. 1–24. John Wiley & Sons Inc, New York.
3. Rossmann, M.G., Moras, D. & Olsen, K.W. (1974) Chemical and biological evolution of a nucleotide-binding protein. *Nature* **250**, 194–199.
4. Kho, R., Baker, B.L., Newman, J.V., Jack, R.M., Sem, D.S., Villar, H.O. & Hansen, M.R. (2003) A path from primary protein sequence to ligand recognition. *Proteins Struct. Func. Genet.* **50**, 589–599.
5. Hektor, H.J., Kloosterman, H. & Dijkhuizen, L. (2002) Identification of a magnesium-dependent NAD(P)(H)-binding domain in the nicotinoprotein methanol dehydrogenase from *Bacillus methanolicus*. *J. Biol. Chem.* **277**, 46966–46973.
6. Entsch, B. & van Berkel, W.J.H. (1995) Structure and mechanism of para-hydroxybenzoate hydroxylase. *FASEB J.* **9**, 476–483.
7. Brunhuber, N.M. & Blanchard, J.S. (1994) The biochemistry and enzymology of amino acid dehydrogenases. *Crit. Rev. Biochem. Mol. Biol.* **29**, 415–467.
8. Kavanagh, K.L., Klimacek, M., Nidetzky, B. & Wilson, D.K. (2003) The structure of xylose reductase bound to NAD^+ and the basis for single and dual cosubstrate specificity in family 2 aldo-keto reductases. *Biochem. J.* **373**, 319–326.
9. Morandi, P., Valzasina, B., Colombo, C., Curti, B. & Vanoni, M.A. (2000) Glutamate synthase: identification of the NADPH-binding site by site-directed mutagenesis. *Biochemistry* **39**, 727–735.
10. Wang, H., Lei, B. & Tu, S.C. (2000) *Vibrio harveyi* NADPH-FMN oxidoreductase arg203 as a critical residue for NADPH recognition and binding. *Biochemistry* **39**, 7813–7819.
11. Perozich, J., Kuo, I., Lindahl, R. & Hempel, J. (2001) Coenzyme specificity in aldehyde dehydrogenase. *Chem. Biol. Interact.* **130–132**, 115–124.

12. Ratnam, K., Ma, H. & Penning, T.M. (1999) The arginine 276 anchor for NADP(H) dictates fluorescence kinetic transients in 3 alpha-hydroxysteroid dehydrogenase, a representative aldo-keto reductase. *Biochemistry* **38**, 7856–7864.
13. Hermoso, J.A., Mayoral, T., Faro, M., Gomez-Moreno, C., Sanz-Aparicio, J. & Medina, M. (2002) Mechanism of coenzyme recognition and binding revealed by crystal structure analysis of ferredoxin-$NADP^+$ reductase complexed with $NADP^+$. *J. Mol. Biol.* **319**, 1133–1142.
14. Dohr, O., Paine, M.J.I., Friedberg, T., Roberts, G.C.K. & Wolf, C.R. (2001) Engineering of a functional human NADH-dependent cytochrome P450 system. *Proc. Natl Acad. Sci. USA* **98**, 81–86.
15. Scrutton, N.S., Berry, A. & Perham, R.N. (1990) Redesign of the coenzyme specificity of a dehydrogenase by protein engineering. *Nature* **343**, 38–43.
16. Chen, R., Greer, A. & Dean, A.M. (1996) Redesigning secondary structure to invert coenzyme specificity in isopropylmalate dehydrogenase. *Proc. Natl Acad. Sci. USA* **93**, 12171–12176.
17. Holmberg, N., Ryde, U. & Bulow, L. (1999) Redesign of the coenzyme specificity in 1-lactate dehydrogenase from *Bacillus stearothermophilus* using site-directed mutagenesis and media engineering. *Protein Eng.* **12**, 851–856.
18. Serov, A.E., Popova, A.S., Fedorchuk, V.V. & Tishkov, V.I. (2002) Engineering of coenzyme specificity of formate dehydrogenase from *Saccharomyces cerevisae*. *Biochem. J.* **367**, 841–847.
19. Banta, S., Swanson, B.A., Wu, S., Jarnagin, A. & Anderson, S. (2002) Alteration of the specificity of the cofactor-binding pocket of *Corynebacterium* 2,5-diketo-D-gluconic acid reductase A. *Protein Eng.* **15**, 131–140.
20. Eppink, M.H.M., Overkamp, K.M., Schreuder, H.A. & Van Berkel, W.J.H. (1999) Switch of coenzyme specificity of *p*-hydroxybenzoate hydroxylase. *J. Mol. Biol.* **292**, 87–96.
21. Penning, T.M. & Jez, J.M. (2001) Enzyme redesign. *Chem. Rev.* **101**, 3027–3046.
22. Kamerbeek, N.M., Janssen, D.B., van Berkel, W.J.H. & Fraaije, M.W. (2003) Baeyer-Villiger monooxygenases, an emerging family of flavin-dependent biocatalysts. *Adv. Synth. Catal.* **345**, 1–12.
23. Willetts, A. (1997) Structural studies and synthetic applications of Baeyer-Villiger monooxygenases. *Trends Biotechnol.* **15**, 55–62.
24. Fraaije, M.W., Kamerbeek, N.M., van Berkel, W.J.H. & Janssen, D.B. (2002) Identification of a Baeyer-Villiger monooxygenase sequence motif. *FEBS Lett.* **518**, 43–47.
25. Brzostowicz, P.C., Walters, D.M., Thomas, S.M., Nagarajan, V. & Rouviere, P.E. (2003) mRNA differential display in a microbial enrichment culture: simultaneous identification of three cyclohexanone monooxygenases from three species. *Appl. Environ. Microbiol.* **69**, 334–342.
26. Van Beilen, J.B., Mourlane, F., Seeger, M.A., Kovac, J., Li, Z., Smits, T.H., Fritsche, U. & Witholt, B. (2003) Cloning of Baeyer-Villiger monooxygenases from *Comamonas*, *Xanthobacter* and *Rhodococcus* using polymerase chain reaction with highly degenerate primers. *Environ. Microbiol.* **5**, 174–182.
27. Wierenga, R.K., Terpstra, P. & Hol, W.G. (1986) Prediction of the occurrence of the ADP-binding beta alpha beta-fold in proteins, using an amino acid sequence fingerprint. *J. Mol. Biol.* **187**, 101–107.
28. Vallon, O. (2000) New sequence motifs in flavoproteins: evidence for common ancestry and tools to predict structure. *Proteins Struct. Funct. Genet.* **38**, 95–114.
29. Walsh, C.T. & Chen, Y.-C.J. (1988) Enzymic Baeyer-Villiger oxidations by flavin-dependent monooxygenases. *Angew. Chem. Int. Ed.* **27**, 333–343.
30. Mihovilovic, M.D., Muller, B. & Stanetty, P. (2002) Monooxygenase-mediated Baeyer-Villiger oxidations. *Eur. J. Org. Chem.* **22**, 3711–3730.
31. Panke, S., Held, M., Wubbolts, M.G., Witholt, B. & Schmid, A. (2002) Pilot-scale production of (*S*)-styrene oxide by recombinant *Escherichia coli* synthesizing styrene monooxygenase. *Biotechnol. Bioeng.* **80**, 33–41.
32. Alphand, V., Carrea, G., Wohlgemuth, R., Furstoss, R. & Woodley, J.M. (2003) Towards large-scale synthetic applications of Baeyer-Villiger monooxygenases. *Trends Biotechnol.* **21**, 318–323.
33. Lundquist, R. & Olivera, B.M. (1971) Pyridine nucleotide metabolism in *Escherichia coli*. I. Exponential growth. *J. Biol. Chem.* **246**, 1107–1116.
34. Kamerbeek, N.M., Olsthoorn, A.J.J., Fraaije, M.W. & Janssen, D.B. (2003b) Substrate specificity and enantioselectivity of 4-hydroxyacetophenone monooxygenase. *Appl. Environ. Microbiol.* **69**, 419–426.
35. Kamerbeek, N.M., Moonen, M.J., Van Der Ven, J.G., Van Berkel, W.J.H., Fraaije, M.W. & Janssen, D.B. (2001) 4-Hydroxyacetophenone monooxygenase from *Pseudomonas fluorescens* ACB. A novel flavoprotein catalyzing Baeyer–Villiger oxidation of aromatic compounds. *Eur. J. Biochem.* **268**, 2547–2557.
36. Suh, J.K., Poulsen, L.L., Ziegler, D.M. & Robertus, J.D. (1999) Lysine 219 participates in NADPH specificity in a flavin-containing monooxygenase from *Saccharomyces cerevisiae*. *Arch. Biochem. Biophys.* **372**, 360–366.
37. Reference withdrawn.
38. Doig, S.D., O'Sullivan, L.M., Patel, S., Ward, J.M. & Woodley, J.M. (2001) Large scale production of cyclohexanone monooxygenase from *Escherichia coli* TOP10 pQR239. *Enz. Microbiol. Techn.* **28**, 265–274.
39. Bradford, M.M. (1976) A rapid and sensitive method for the quantitation of microgram quantities of protein utilizing the principle of protein-dye binding. *Anal. Biochem.* **72**, 248–254.
40. Sheng, D., Ballou, D.P. & Massey, V. (2001) Mechanistic studies of cyclohexanone monooxygenase: chemical properties of intermediates involved in catalysis. *Biochemistry* **40**, 11156–11167.
41. Lennon, B.W., Williams, C.H. Jr & Ludwig, M.L. (2000) Twists in catalysis: alternating conformations of *Escherichia coli* thioredoxin reductase. *Science* **289**, 1190–1194.
42. Danielson, U.H., Jiang, F., Hansson, L.O. & Mannervik, B. (1999) Probing the kinetic mechanism and coenzyme specificity of glutathione reductase from the cyanobacterium *Anabaena* PCC 7120 by redesign of the pyridine-nucleotide-binding site. *Biochemistry* **38**, 9254–9563.
43. Nakanishi, M., Kakumoto, M., Matsuura, K., Deyashiki, Y., Tanaka, N., Nonaka, T., Mitsui, Y. & Hara, A. (1996) Involvement of two basic residues (Lys-17 and Arg-39) of mouse lung carbonyl reductase in NADP(H)-binding and fatty acid activation: site-directed mutagenesis and kinetic analyses. *J. Biochem.* **120**, 257–263.
44. Wilson, D.K., Kavanagh, K.L., Klimacek, M. & Nidetzky, B. (2003) The xylose reductase (AKR2B5) structure: homology and divergence from other aldo-keto reductases and opportunities for protein engineering. *Chem. Biol. Interact.* **143–144**, 515–521.
45. Copley, R.R. & Barton, G.J. (1994) A structural analysis of phosphate and sulphate binding sites in proteins. Estimation of propensities for binding and conservation of phosphate binding sites. *J. Mol. Biol.* **242**, 321–329.
46. Barber, M.J., Desai, S.K. & Marohnic, C.C. (2001) Assimilatory nitrate reductase: lysine 741 participates in pyridine nucleotide binding via charge complementarity. *Arch. Biochem. Biophys.* **394**, 99–110.
47. Pai, E.F., Karplus, P.A. & Schulz, G.E. (1988) Crystallographic analysis of the binding of NADPH, NADPH fragments, and

NADPH analogues to glutathione reductase. *Biochemistry* **27**, 4465–4474.
48. Wu, Y.-D. & Houk, K.N. (1993) Theoretical study of conformational features of NAD^+ and NADH analogs: protonated nicotinamide and 1,4-dihydronicotinamide. *J. Org. Chem.* **58**, 2043–2045.
49. You, K.S. (1985) Stereospecificity for nicotinamide nucleotides in enzymatic and chemical hydride transfer reactions. *CRC Crit. Rev. Biochem.* **17**, 313–451.
50. Polshakov, V.I., Biekofsky, R.R., Birdsall, B. & Feeney, J. (2002) Towards understanding the origins of the different specificities of binding the reduced (NADPH) and oxidised ($NADP^+$) forms of nicotinamide adenine dinucleotide phosphate coenzyme to dihydrofolate reductase. *J. Mol. Struct.* **602–603**, 257–267.
51. Ryerson, C.C., Ballou, D.P. & Walsh, C. (1982) Mechanistic studies on cyclohexanone oxygenase. *Biochemistry* **21**, 2644–2655.
52. Stabile, H., Curti, B. & Vanoni, M.A. (2000) Functional properties of recombinant *Azospirillum brasilense* glutamate synthase, a complex iron-sulfur flavoprotein. *Eur. J. Biochem.* **267**, 2720–2730.
53. Fraaije, M.W., Kamerbeek, N.M., Heidekamp, A.J., Fortin, R. & Janssen, D.B. (2004) The prodrug activator EtaA from *Mycobacterium tuberculosis* is a Baeyer-Villiger monooxygenase. *J. Biol. Chem.* **279**, 3354–3360.
54. Manstein, D.J., Massey, V., Ghisla, S. & Pai, E.F. (1988) Stereochemistry and accessibility of prosthetic groups in flavoproteins. *Biochemistry* **27**, 2300–2305.